9. Marangoni Flows

Marangoni flows are those driven by surface gradients. In general, surface tension σ depends on both the temperature and chemical composition at the interface; consequently, Marangoni flows may be generated by gradients in either temperature or chemical composition at an interface. We previously derived the tangential stress balance at a free surface:

$$\boldsymbol{n} \cdot \boldsymbol{T} \cdot \boldsymbol{t} = -\boldsymbol{t} \cdot \boldsymbol{\nabla}\sigma \quad , \tag{9.1}$$

where $\boldsymbol{n}$ is the unit outward normal to the surface, and $\boldsymbol{t}$ is any unit tangent vector. The tangential component of the hydrodynamic stress at the surface must balance the tangential stress associated with gradients in σ. Such Marangoni stresses may result from gradients in temperature or chemical composition at the interface. For a static system, since $\boldsymbol{n} \cdot \boldsymbol{T} \cdot \boldsymbol{t} = 0$, the tangential stress balance equation indicates that: $0 = \boldsymbol{\nabla}\sigma$. This leads us to the following important conclusion:

There cannot be a static system in the presence of surface tension gradients.

While pressure jumps can arise in static systems characterized by a normal stress jump across a fluid interface, they do not contribute to the tangential stress jump. Consequently, tangential surface stresses can only be balanced by viscous stresses associated with fluid motion.

Thermocapillary flows: Marangoni flows induced by temperature gradients $\sigma(T)$.

`Note` that in general $\frac{d\sigma}{dT} < 0$ Why? A warmer gas phase has more liquid molecules, so the creation of surface is less energetically unfavourable; therefore, σ is lower.

Approach Through the interfacial BCs (and $\sigma(T)$'s appearance therein), N-S equations must be coupled

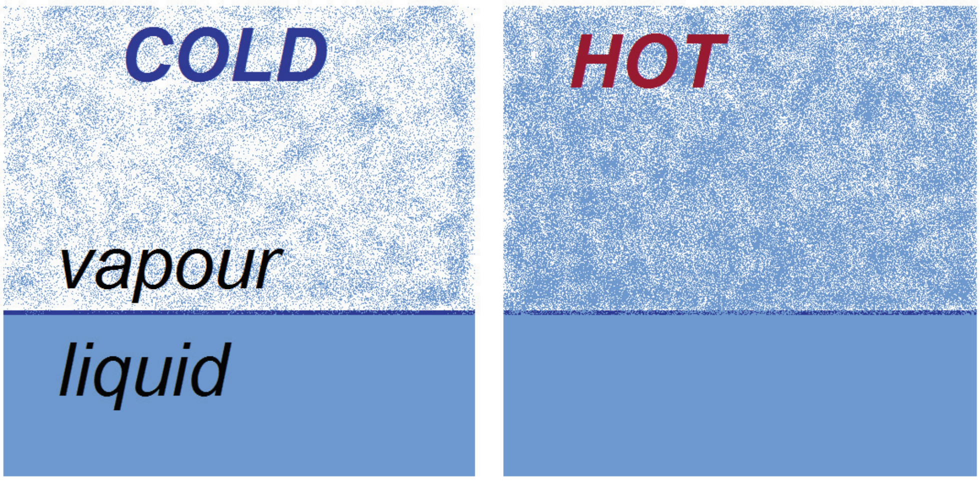

Figure 9.1: Surface tension of a gas-liquid interface decreases with temperature since a warmer gas phase contains more suspended liquid molecules. The energetic penalty of a liquid molecule moving to the interface is thus decreased.

to the heat equation

$$\frac{\partial T}{\partial t} + \boldsymbol{u} \cdot \boldsymbol{\nabla} T = \kappa \nabla^2 T \tag{9.2}$$

Note:

1. the heat equation must be solved subject to appropriate BCs at the free surface. Doing so can be complicated, especially if the fluid is evaporating.

2. Analysis may be simplified when the **Peclet number** $\mathcal{P}e = \frac{Ua}{\kappa} \ll 1$. Nondimensionalize (9.2): $\boldsymbol{x} = a\boldsymbol{x}'$, $t = \frac{a}{U}t'$, $\boldsymbol{u} = U\boldsymbol{u}'$ to get

$$\mathcal{P}e\left(\frac{\partial T'}{\partial t'} + \boldsymbol{u}' \cdot \boldsymbol{\nabla}' T'\right) = \nabla^2 T' \tag{9.3}$$

Note:
$\mathcal{P}e = \mathcal{R}e \cdot \mathcal{P}r = \frac{Ua}{\nu} \cdot \frac{\nu}{\kappa} \ll 1$ if $\mathcal{R}e \ll 1$, so one has $\nabla^2 T = 0$.
The **Prandtl number** $\mathcal{P}r = O(1)$ for many common (e.g. aqeous) fluids.
E.g.1 Thermocapillary flow in a slot (Fig.9.2a)
Surface Tangential BCs $\tau = \frac{\Delta\sigma}{L} = \frac{d\sigma}{dT}\frac{\Delta T}{L} \approx \mu \frac{U}{H}$ viscous stress $U \sim \frac{1}{\mu}\frac{H}{L}\Delta\sigma$.

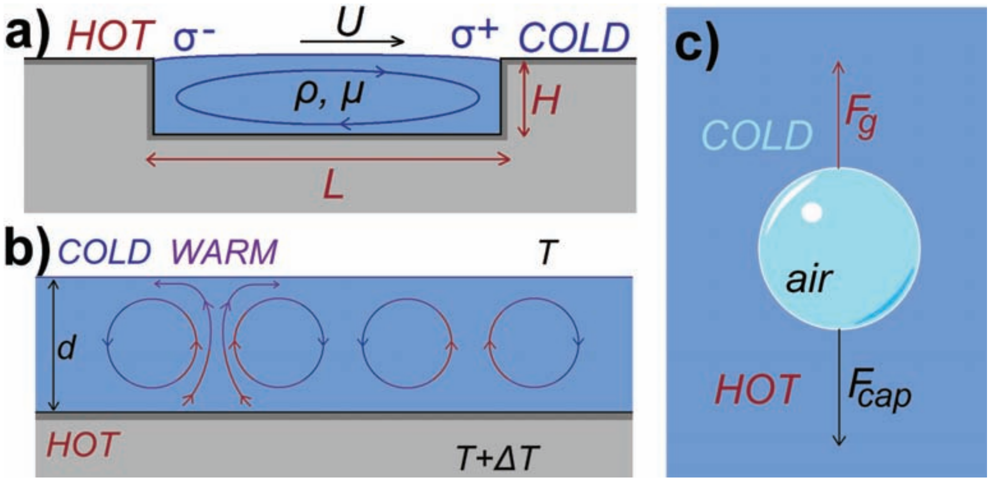

Figure 9.2: **a)** Thermocapillary flow in a slot **b)** Thermal convection in a plane layer **c)** Thermocapillary drop motion.

E.g.2 Thermocapillary Drop Motion (*Young, Goldstein & Block 1962*)
can trap bubbles in gravitational field via thermocapillary forces. (Fig.9.2c).
E.g.3 Thermal Marangoni Convection in a Plane Layer (Fig.9.2b).
Consider a horizontal fluid layer heated from below. Such a layer may be subject to either buoyancy- or Marangoni-induced convection.
Recall: Thermal buoyancy-driven convection (Rayleigh-Bernard) $\rho(T) = \rho_0\,(1 + \alpha(T - T_0))$, where α is the thermal expansivity. Consider a buoyant blob of characteristic scale d. Near the onset of convection, one expects it to rise with a Stokes velocity $U \sim \frac{g\Delta\rho}{\rho}\frac{d^2}{\nu} = \frac{g\alpha\Delta T d^2}{\nu}$. The blob will rise, and so convection will occur, provided its rise time $\tau_{rise} = \frac{d}{U} = \frac{d\nu}{g\alpha\Delta T d^2}$ is less than the time required for it to lose its heat and buoyancy by diffusion, $\tau_{diff} = \frac{d^2}{\kappa}$.

Criterion for Instability: $\frac{\tau_{diff}}{\tau_{rise}} \sim \frac{g\alpha\Delta T d^3}{\kappa\nu} \equiv \mathcal{R}a > \mathcal{R}a_c \sim 10^3$, where $\mathcal{R}a$ is the Rayleigh number.

Note: for $\mathcal{R}a < \mathcal{R}a_c$, heat is transported solely through diffusion, so the layer remains static. For $\mathcal{R}a > \mathcal{R}a_c$, convection arises.
The subsequent behaviour depends on $\mathcal{R}a$ and $\mathcal{P}r$. Generally, as $\mathcal{R}a$ increases, steady convection rolls $\Rightarrow$ time-dependency $\Rightarrow$ chaos $\Rightarrow$ turbulence.

Thermal Marangoni Convection
Arises because of the dependence of σ on temperature: $\sigma(T) = \sigma_0 - \Gamma(T - T_0)$
`Mechanism`:

- Imagine a warm spot on surface $\Rightarrow$ prompts surface divergence $\Rightarrow$ upwelling.
- Upwelling blob is warm, which reinforces the perturbation provided it rises before losing its heat via diffusion.
- Balance Marangoni and viscous stress: $\frac{\Delta\sigma}{d} \sim \frac{\mu U}{d}$
- Rise time: $\frac{d}{U} \sim \frac{\mu d}{\Delta\sigma}$
- Diffusion time $\tau_{diff} = \frac{d^2}{\kappa}$

`Criterion for instability`: $\frac{\tau_{diff}}{\tau_{rise}} \sim \frac{\Gamma \Delta T d}{\mu\kappa} \equiv \mathcal{M}a > \mathcal{M}a_c$, where $\mathcal{M}a$ is the Marangoni number.
`Note`:

1. Since $\mathcal{M}a \sim d$ and $\mathcal{R}a \sim d^3$, thin layers are most unstable to Marangoni convection.
2. Bénard's original experiments performed in millimetric layers of spermaceti were visualizing Marangoni convection, but were misinterpreted by Rayleigh as being due to buoyancy $\Rightarrow$ not recognized until *Block (Nature 1956)*.
3. *Pearson (1958)* performed stability analysis with flat surface $\Rightarrow$ deduced $\mathcal{M}a_c = 80$.
4. *Scriven & Sternling (1964)* considered a deformable interface, which renders the system unstable at all $\mathcal{M}a$. Downwelling beneath peaks in Marangoni convection, upwelling between peaks in Rayleigh-Bénard convection (Fig. 9.3a).
5. *Smith (1966)* showed that the destabilizing influence of the surface may be mitigated by gravity. Stability Criterion: $\frac{d\sigma}{dT}\frac{dT}{dz} < \frac{2}{3}\rho g d \Rightarrow$ thin layers prone to instability.

`E.g.4` **Marangoni Shear Layer** (Fig. 9.3)
Lateral $\nabla\theta$ leads to Marangoni stress $\Rightarrow$ shear flow. The resulting $T(x, y)$ may destabilize the layer to

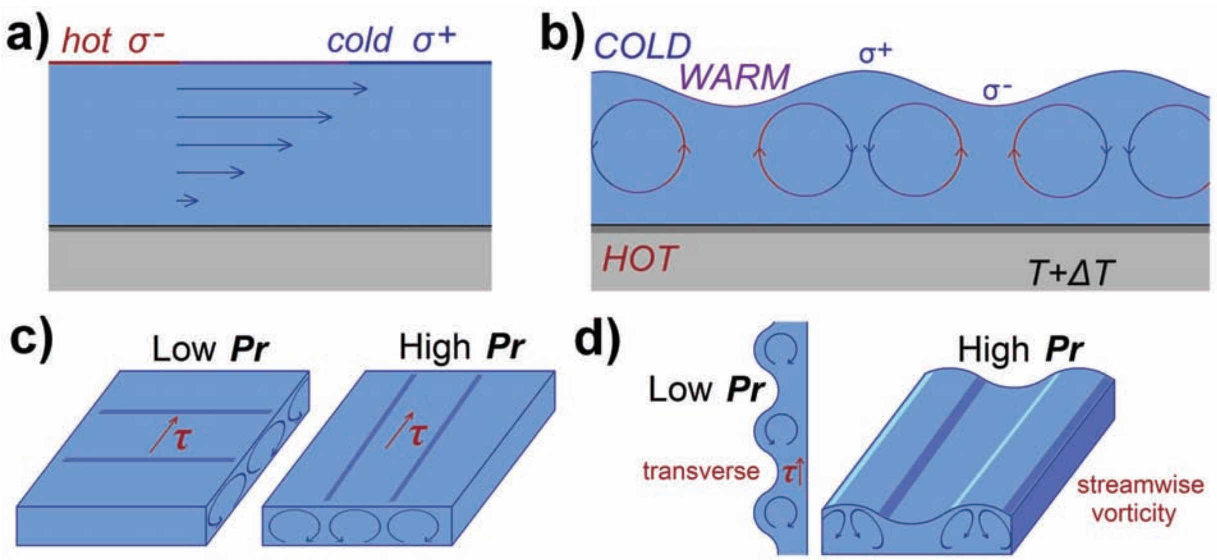

Figure 9.3: **a)** Marangoni convection in a shear layer may lead to transverse surface waves or streamwise rolls **(c)**. Surface deflection may accompany both instabilities **(b,d)**.

Marangoni convection.
Smith & Davis (1983ab) considered the case of flat free surface. System behaviour depends on $\mathcal{P}r = \nu/\kappa$.
Low $\mathcal{P}r$: Hydrothermal waves propagate in direction of τ.
High $\mathcal{P}r$: Streamwise vortices (Fig. 9.3c).
Hosoi & Bush (2001) considered a deformable free surface (Fig. 9.3d)

`E.g.5` **Evaporatively-driven convection**
e.g. for an alcohol-H_2O solution, evaporation affects both the alcohol concentration c and temperature θ. The density $\rho(c, \theta)$ and surface tension $\sigma(c, \theta)$ are such that $\frac{\partial \rho}{\partial \theta} < 0$, $\frac{\partial \rho}{\partial c} < 0$, $\frac{d\sigma}{d\theta} < 0$, $\frac{d\sigma}{dc} < 0$. Evaporation results in surface cooling and so may generate either Rayleigh-Bénard or Marangoni thermal convection. Since it also induces a change in surface chemistry, it may likewise generate either $Ra - B$ or Marangoni chemical convection.

`E.g.6` **Coffee Drop**
Marangoni flows are responsible for the ring-like stain left by a coffee drop.

- coffee grounds stick to the surface
- evaporation leads to surface cooling, which is most pronounced near the edge, where surface area per volume ratio is highest
- resulting thermal Marangoni stresses drive radial outflow on surface $\Rightarrow$ radial ring

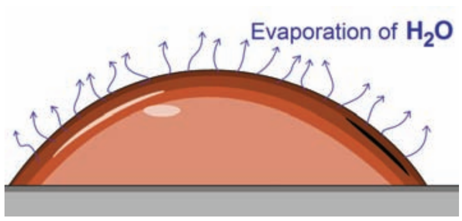

Figure 9.4: Evaporation of water from a coffee drop drives a Marangoni flow.